Results in Physics 39 (2022) 105703

Contents lists available at ScienceDirect

Results in Physics

journal homepage: www.elsevier.com/locate/rinp

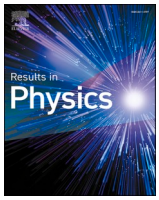

Tailoring the spatial-dependent Rashba parameter and spin fluctuations in nanomaterials for improved spin-FET functionality

C.H. Wong [a,c,d,*], R. Lortz [b], C.Y. Tang [c], A.F. Zatsepin [a]

[a] Institute of Physics and Technology, Ural Federal University, Yekaterinburg, Russia
[b] Department of Physics, The Hong Kong University of Science and Technology, Clear Water Bay, Hong Kong
[c] Department of Industrial and Systems Engineering, The Hong Kong Polytechnic University, Hung Hom, Kowloon, Hong Kong
[d] Research Institute for Advanced Manufacturing, The Hong Kong Polytechnic University, Hung Hom, Kowloon, Hong Kong

ARTICLE INFO

Keywords:
Rashba effect
spintronics
Monte Carlo simulation

ABSTRACT

The spatial fluctuation of the Rashba parameter has been a major issue in the development of state-of-the-art spintronic nanodevices. Since stable spin-precession is of vital importance in the spin field-effect transistor (spin-FET), we have developed a Monte Carlo model to justify that the local E-field of heavy dopants is the origin of the fluctuating Rashba parameter. To maintain a stable drain current in spin-FETs, we study how the size of lattice, doping condition, E-field screening, exchange interaction and temperature influence the Rashba interaction in nanomaterials. Our Monte Carlo model can predict the Rashba effect of Graphene/Nickel(1 1 1) substrate at room temperature and presents a path to enhance the Rashba interactions via proximity coupling. More importantly, we have discovered a dip-like structure in the Rashba parameter that strongly scatters the spin states, and we have figured out how to suppress spin fluctuations in the semiconductor channel. Our results are important for the development of the next generation of spin transistors.

Introduction

The development of a room-temperature Rashba material is a challenging problem. The discoveries of giant Rashba effect in BiTeI, GeTe and in a number of low-dimensional materials give hope that spintronic devices such as spin-filters, spin-FETs, etc. can be operated at high temperatures[1–4]. Spin transistors are a hot research topic due to their superior performances, such as high-speed operation and low switching energy [1–4]. Moreover, the static power dissipation of spin transistors is rare compared to charge-based transistors, which is expected to be a solution to the serious power dissipations in CMOS logical circuits [1–4].

A spin-FET consists of a two-dimensional semiconductor sandwiched between two ferromagnetic contacts (i.e. source and drain)[5]. The ferromagnetic source sends spin-polarized electrons into the semiconductor channel, with spin precession triggered by spin–orbit coupling [6]. However, before the spin-FET can be put into practice, scientists must overcome a major technological challenge, namely, maintaining spin direction as electrons move through the semiconductor channel, where electrons are always scattered into other spin states after a short distance. Spin transport from the semiconductor channel is allowed when the spin of an electron is parallel to the drain magnetization [6]. In other words, maintaining a uniform rate of spin-precession in the semiconductor channel is critical for generating a stable output current in the spin-FET.

In the presence of the Rashba spin-orbital interaction, there is always a momentum-dependent splitting of spin under an external electric field perpendicular to the 2D plane [3,4]. The phenomenon of spin-splitting without the need of an external magnetic field in the Rashba system is credited to the strong spin–orbit coupling and the asymmetric potential of crystals [3,4]. However, the chaotic pattern of the Rashba parameter has been observed experimentally in nanomaterials composed of heavy elements although the concentration is only 1.8% [7], which makes stable drain current in the spin-FETs unlikely. Suppression of the randomization of the Rashba parameter is possible when the semiconductor channel is made of graphene, which has a low atomic number. Although the spin-orbital coupling of graphene is weak, a strong magnetic interaction between Graphene and Nickel(1 1 1) substrate [8,9,10] is observed, where a ferromagnetic proximity effect can enhance the Rashba effect [8,9] of graphene up to room temperature.

For the electrons under the Rashba effect, the berry curvature acts as an effective magnetic field to produce a Lorentz-like force $F = q(v_x \times B_{Rashba})$ that bends the trajectory of an electron with horizontal veloc-

* Corresponding author.
E-mail address: roych.wong@polyu.edu.hk (C.H. Wong).

https://doi.org/10.1016/j.rinp.2022.105703
Received 31 March 2022; Received in revised form 24 May 2022; Accepted 5 June 2022
Available online 8 June 2022

ity$v_{\pm x}$, thereby resulting in an anomalous velocity [4]. This effective magnetic field along the y-axis is expressed as$B_{Rashba} = \frac{2\alpha k_F}{g\mu_B}$, where the Rashba coefficientα, the Fermi wavevectork_F, the g-factor of electron g and the permeability of the medium μ_B are defined [4,11]. An electron with charge q experiences an additional acceleration term triggered by the in-plane effective magnetic field. If the effective magnetic field is randomly distributed along the sample surface, the additional acceleration of electrons varies from space to space and the local rate of spin-precession becomes unpredictable. Although a Quantum Monte Carlo model can describe the Rashba effect at a reasonable level [12], it is not specifically designed for the random Rashba interactions. Fortunately, the Rashba spin-orbital interaction alters the trajectory of electrons in a manner similar that the Magnus force distorts the trajectory of a rotating particle in classical mechanics [4]. This motivates us to test whether our semi-classical Monte Carlo approach being capable of predicting the uniformness of Rashba-type spin-momentum locking (with or without dopants). If the Rashba effect is not uniform along the sample surface, we simulate the spatial pattern of the Rashba effect to suppress the non-uniformity of the Rashba interaction by parametric studies. All simulation results are presented in physical units.

Methods

Hamiltonian

There are 8192 electrons in a square box. The Hamiltonian is listed below.

$$H = \sum_{<ij>}\left[E_{KE} + E_{Rashba} + E_{exchange} + E_{dopant}\right]$$

The kinetic energy, Rashba potential, exchange energy and doping energy are $E_{KE} = \frac{\hbar^2 k^2 R_{KE}^2}{2m}$ [11], $E_{Rashba} \sim \alpha k R_{KE}\delta(S_\pm)$ [4], $E_{ex} = J_0 e^{-\frac{|r_i - r_j|}{r_o}} S_i \cdot S_j$ [11,13], and $E_{dopant} \sim -\frac{Z_{dope} q^2}{4\pi\varepsilon d}\frac{R_{screen}}{B_{max}}$, respectively. R_{KE} and R_{screen} are the random numbers between 0 and 1. $\hbar$ refers to Planck's constant. α is the Rashba coefficient and the modified wavevector of electrons due to the Rashba spin-orbital coupling is $k_{SO} = \frac{m\alpha}{\hbar^2}$[19]. The locations of the i^{th} and j^{th} electrons in the XY plane are abbreviated as $\mathbf{r_i}$ and $\mathbf{r_j}$, respectively. The exchange interaction is valid among the four nearest neighbors. The electrons are separated by r_o on average where r_o is converted from the Fermi energy in Table 1 [9,15,22]. The Fermi energy and the total number of electrons determine the size of the simulation box (23 nm × 23 nm). The role of the delta function $\delta(S_\pm) = \mp 1$ is to trigger spin - momentum locking [4], where the electron with a spin-up S_+ (spin-down S_-) state travels to + x (-x) direction [16]. The eigenvalue of the spin operator is $S_\pm = \pm\frac{\hbar}{2}$. The average electron-dopant separation is d. The permittivity and Coulomb charge are ε and q, respectively. The Rashba coefficient at finite temperature T is reported to be $\alpha' = \alpha + 1.75x10^{-4}T$[20,21]. The calibrated random number B_{max} controls the effectiveness of E-field screening.

Due to the experimental fact that the Rashba coefficient of the InSb-based material shows spatial fluctuations[7], we set the atomic number of heavy dopants to$Z_{dope} = 50$ (unless otherwise specified) in order to approximately match the atomic number of In or Sb. The randomly distributed dopants occupy ~ 1% area of the simulation box.

Table 1
The simulation parameters [9,15,22] of the Graphene/Nickel(1 1 1) substrate (unless otherwise specified).

Fermi energy E_F	~4 eV [15]
Rashba wavevector k_{SO} (Å)	0.08 $Å^{-1}$ [9]
Exchange energy J_o	−0.012 eV [15]
Scattering time t	20 fs [22]
Rashba coefficient $\alpha_{initial}$	1 eVÅ [9]
The mass of electron m	$9.11x10^{-31}$kg
The size of the simulation box	~20 nm × ~ 20 nm
Doping concentration	~1%

Effective wavevectors

The electronic properties of graphene are probed by first-principal calculations based on the density functional theory implemented in WIEN2k ab-initio simulation program. The Generalized Gradient Approximation (GGA) in the scheme of Perdew-Burke-Ernzerhof (PBE) is used to determine the exchange interaction J_0 of Graphene/Nickel (1 1 1) composite. Our computed value of J_0 is −0.012 eV [15]. The cut-off energy point is 329.3 eV. The SCF tolerance is $2x10^{-6}$eV/atom. The maximum SCF is 100. The separation of k point is 0.05 $Å^{-1}$. In order to use a square lattice to describe the dynamic of electron in a hexagonal lattice approximately, we apply Density Functional Theory (DFT) at GGA-PBE level [16] to obtain the effective wavevectors $\langle k_x\rangle = \frac{1.06k}{\sqrt{2}} =$ 0.62 $Å^{-1}$ and $\langle k_y\rangle = \frac{0.94k}{\sqrt{2}} = 0.54$ $Å^{-1}$, which correspond to the purple and red regions in Fig. 1, respectively. The wavevector of electrons in the XY plane is $k = \sqrt{k_x^2 + k_y^2}$. The S_+ and S_- electrons are located within $-L_x <= X <= L_x$ and $-L_y <= Y <= L_y$.

Definition of a uniform Rashba effect

The following assumptions are made:

(1) The spin-momentum locking is secured for all electrons.
(2) The effective magnetic field is uniform along the sample surface.

Description of the algorithm

Step 1: Apply initial condition to load 4096 S_+ and 4096 S_- electrons to the sample, respectively. Randomize the location of electrons at each temperature. If dopants exist, they are distributed in a random manner.

Step 2: Read the trial states (spin, wavevector, location) of the randomly selected electron.

Step 3: Generate a random number ($0 \leqslant R_1 \leqslant 1$). If R_1 is greater than 0.5, the selected electron reverses the direction of spin. Otherwise, the trial spin state retains.

Step 4: Create another random number ($0 \leqslant R_2 \leqslant 1$) to control the direction of motion. If R_2 is greater than 0.5, the selected electron moves towards + x direction [14]. Otherwise, the electron moves to the -x direction.

Step 5: Check whether the selected electron locks the spin and momentum or not. If locked, the trial wavevectors are $k_{\pm x}^{trial} = \left(\langle k_x\rangle \pm \frac{k_{SO}}{\sqrt{2}}\right)$ and$k_{\pm y}^{trial} = \left(\langle k_y\rangle \pm \frac{k_{SO}}{\sqrt{2}}\right)$. Otherwise, k_{SO} equals to 0. The selected elec-

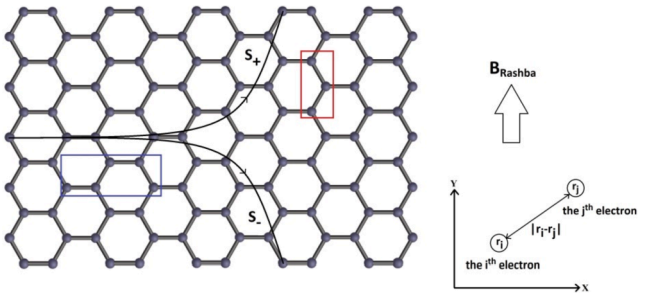

Fig 1. Graphene has a hexagonal honeycomb structure. For clarity reasons, only the local area of graphene is drawn. The effective wavevectors in the purple and red regions are directly obtained from our DFT calculations. The spin-splitting phenomenon (spin-up state: S_+, spin-down state: S_-) under the effective magnetic field B_{Rashba} is illustrated. Berry curvature behaves as an effective magnetic field that creates a Lorentz-like force.

tron may choose k_{+y}^{trial} or k_{-y}^{trial} in equal probability.

Step 6: When the effective magnetic field is valid, the additional velocity of an electron in classical mechanics,$v_y = q(v_x \times B_{Rashba})\tau/m$, may be approximated to$v_y \sim (-\alpha/\hbar)z \times \sigma_{\pm}$, where $\sigma_{\pm}$ is the vector of Pauli spin matrices [4].

Step 7: Interpret the trial displacement of the selected electron. i.e. $\delta L_x = v_x\tau/m$ and$\delta L_y = v_y\tau/m$. No trial displacement can be larger than the size of the simulation box.

Step 8: Generate another random number$0 \leqslant R_3 \leqslant 0.5$.

Step 9: If $\Delta H < 0$ or$R_3 < \frac{1}{1+e^{\Delta H/k_BT}}$, the trial states ($S_{\pm}$,$k_{\pm}R$, δL) are accepted. Otherwise, return to step 2. On the other hand, if the selected electron shares the same trial states with another electron, return to Step 2.

Step 10: Select another electron randomly until the system reaches equilibrium (~1600000 Monte Carlo steps) at each temperature.

Step 11: To check the spin-momentum locking (SML) at equilibrium, the simulation box is divided into 100 regions in equal area. In each region, observe the probability of spin-momentum locking $P_{SML} = \frac{N_{SM}}{N_{total}}$ where N_{SM} is the total number of SM-locked electrons and N_{total} is the total number of electrons in the system.

Step 12: Calculate the local Rashba coefficient per region, i.e.$\alpha_{local} \sim \alpha_{initial} P_{SML}$

Results

Fig. 2 shows the spatial distribution of electrons in the Graphene/Nickel(1 1 1) substrate at 1 K. Although one S_+ electron is noticed in the lower half-plane, most of the electrons there correspond to the S_- state. Only ~ 40 electrons escape from the Rashba edges at 1 K, where the probability of generating a uniform Rashba effect is ~ 99%. In a real sample, there are many more electrons, since we only use ~ 8000 electrons in our system.

To examine how thermal energy pales the Rashba spin-splitting phenomenon, we show in Fig. 3a how the uniformity of the Rashba effect is faded upon heating. When the composite is at 1 K, the Graphene/Nickel (1 1 1) substrate ($\alpha_{initial}$ = 1eVÅ) exhibits a uniform Rashba effect with the probability of ~ 0.99. The probability (black curve) in Fig. 3a remains at ~ 87% even if the composite is at 300 K. However, the probability function is very sensitive to the $\alpha_{initial}$. The Graphene/strained Nickel (1 1 1) substrate ($\alpha_{initial}$ = 0.1eVÅ) struggles to maintain a uniform Rashba effect at 300 K, with the evidence of$P(Rashba) =$ 0.25. We study the coupling factor between the Rashba spin-orbital coupling and ferromagnetic proximity interaction in Fig. 3b. Although these two exchange couplings have the same average strength, electrons exposed to a non-uniform ferromagnetic proximity interaction reinforce the Rashba spin-splitting phenomenon.

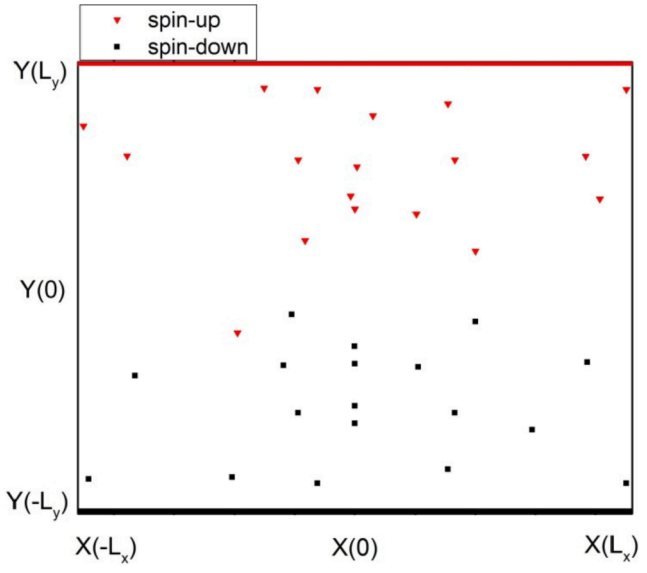

Fig. 2. At equilibrium, the S_+ and S_- electrons accumulate on the upper and lower edges (or Rashba edges for short) at 1 K, respectively.

In Fig. 4a we plot the local Rashba coefficient along the sample surface. A weakening of the Rashba effect by ~ 25% is observed at X ~ 0, which is interpreted from the local probability of spin-momentum locking. Fig. 4b shows that the introduction of ~ 5% vacancies in the two columns near X ~ 0, i.e.$\frac{-L_x}{10} \leqslant x \leqslant \frac{L_x}{10}$, improves the uniformity of the Rashba interaction along the x-axis. The size effect of the local Rashba coefficient is studied in Fig. 5. Reducing the dimensions from 64 × 64 to 32 × 32 reduces the local Rashba coefficient at X ~ 0 more sharply. In the box of 32 × 32, the dip-like feature is more pronounced.

We show step by step how the heavy dopants randomize the Rashba parameter. The fluctuation of the Rashba parameter is related to how strongly the electrons shield the E-field emitted by heavy dopants. When the spin-polarized electrons are injected from –L$_x$ to + L$_x$ in the presence of 1% heavy dopants, the spin precession is weakened by ~ 60% in the green–blue region as plotted in Fig. 6a. After setting a smaller B$_{max}$ in Fig. 6b, the introduction of ~ 1% dopant in the Graphene/Nickel(1 1 1) substrate randomizes the local Rashba coefficient throughout the sample, with the average Rashba coefficient dropping to ~ 0.4$\alpha_{initial.}$ On the other hand, the atomic number of dopants also affects the spatial pattern of the Rashba parameter. For example, as shown in Fig. 7a, the uniformity of the Rashba effect is only slightly affected by the use of a light dopant. The local Rashba coefficients are always stronger at X ~ ±L$_x$. The data in Figs. 2 to 7 do not show any noticeable differences when we rotate the sample by 90 degrees by setting the effective wavevectors to $\langle k_x \rangle = \frac{0.94k}{\sqrt{2}}$ and$\langle k_y \rangle = \frac{1.06k}{\sqrt{2}}$, respectively.

Discussion

Although we initially randomize the location and the spin state of electrons, our Monte Carlo approach is able to produce a strong spin-splitting phenomenon at low temperatures, as demonstrated in Fig. 2. Unexpectedly, there is one spin-up state in the lower half-plane in Fig. 2. This is due to thermal fluctuations determined by the competition between the random number R_3 and the Fermi-Dirac factor$\frac{1}{1+e^{\Delta H/k_BT}}$, analogous to the Boltzmann factor [13,14]. At low temperatures the trial states for $\Delta H > 0$ are rarely accepted because the mean occupation number of the Fermi-Dirac distribution is usually smaller than the random numberR_3. In contrast, at high temperatures, the random number R_3 is usually smaller than the Fermi-Dirac factor, which allows the spin-polarized electrons to accept the trial states more easily [4]. We set $0 \leqslant R_3 \leqslant 0.5$ instead of $0 \leqslant R_3 \leqslant 1$ because the mean occupation number above the Fermi level never exceeds 0.5 above 0 K. In classical mechanics, the ground-state energy H_{GND} at 0 K is zero. The H_{GND} term vanishes in the Boltzmann factor $e^{\Delta H/k_BT}$ because the calculation of ΔH cancels out two H_{GND} terms when a classical particle is excited from $H_1 + H_{GND}$ to$H_2 + H_{GND}$. Similarly, from a quantum mechanical point of view, these two ground-state energies ($H_{GND} = E_F$) cancel each other when ΔH is estimated. As a result, the Fermi energy does not appear in the Fermi-Dirac factor.

Fig. 3a confirms that our Monte Carlo algorithm works well for predicting the room-temperature Rashba effect in Graphene / Nickel (1 1 1) substrate [9]. Our Hamiltonian is suitable for studying the Rashba effect of carbon-based materials because the atomic number of carbon (Z = 6) does not exhibit strong intrinsic spin–orbit coupling [11], which allows us to describe the Hamiltonian with only four terms. However, not all 2D materials exhibit the Rashba effect at room temperature in the presence of ferromagnetic proximity coupling [4,9]. One of the reasons for this can be seen in Fig. 3b, where the Rashba spin splitting is enhanced when ferromagnetic fluctuations occur. When the nickel substrate is replaced by a stronger ferromagnet, the Rashba spin-orbital

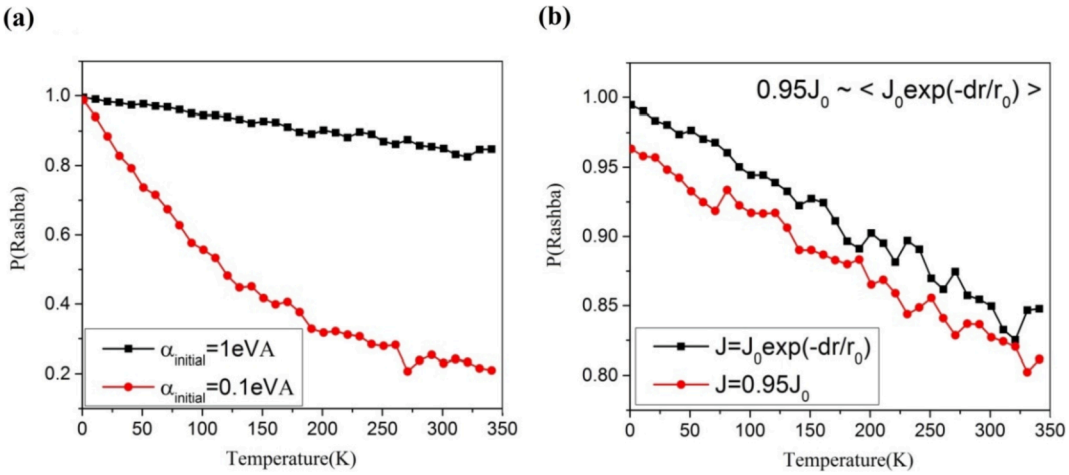

Fig. 3. (a) Probability of formation of a uniform Rashba effect,*P*(*Rashba*), in Graphene/Nickel (1 1 1) substrate as a function of temperature. The strained substrate ($\alpha_{initial}$ = 0.1eVÅ) weakens the exchange interaction and softens the $\alpha_{initial}$ (b) The probability of producing a uniform Rashba effect in a Graphene/Nickel (1 1 1) substrate is studied at different proximity interactions. The red curve refers to the situation where the ferromagnetic proximity interaction propagates constantly to graphene. The black curve refers to a more realistic case where the ferromagnetic proximity interaction fluctuates.

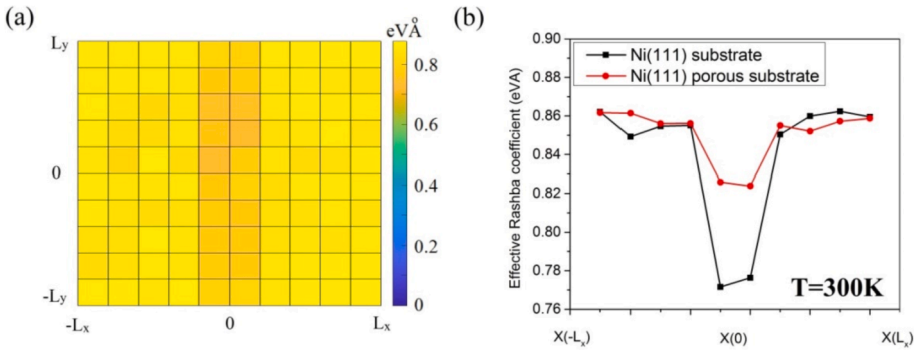

Fig. 4. The real-space patterns of the Rashba coefficient in the Graphene-based materials at 300 K. (a) The $\alpha_{initial}$ of the Graphene/Nickel(1 1 1) substrate is 1eVÅ. (b) By averaging the local Rashba coefficients column-by-column, the effective Rashba coefficient is plotted along the x-axis.

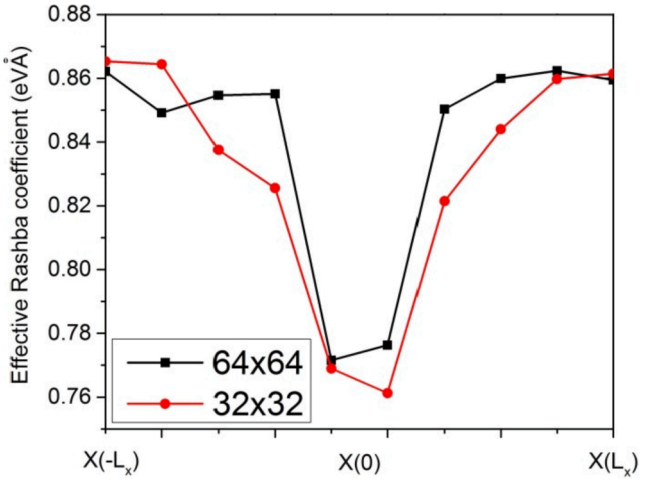

Fig. 5. The spatial pattern of the Rashba parameter depends on the size of the simulation box. The $\alpha_{initial}$ is 1eVÅ. A more pronounced dip-like feature is observed in a smaller simulation box.

coupling cannot be guaranteed to be enhanced because the rate of exchange fluctuations may be slow. To enhance the Rashba spin-orbital coupling via proximity interactions, we need to consider the rate of exchange fluctuations, rather than only tuning the ferromagnetic strength of the substrate.

Although an isolated graphene is not magnetic, a strong exchange interaction occurs with a Graphene/Nickel (1 1 1) substrate [15]. Our DFT simulation shows that the exchange coupling of Graphene/ Nickel (1 1 1) substrate is 12 meV, which is comparable to the exchange coupling of the isolated Nickel (1 1 1) substrate at 14 meV [15,16]. Therefore, it is reasonable to include the exchange term in the Hamiltonian.

Fig. 4b demonstrates that the introduction of a tiny amount of vacancies in the central region improves the uniformity of the Rashba interaction along the x-axis, since the vacancies cause a higher rate of exchange fluctuation and presumably enhance the Rashba spin-splitting. The number of vacancies in the central region is limited to 5%. Otherwise, it may trigger frustrated spin systems, analogous to the spin frustration in the overdoped Ising model [17,23]. Fig. 5 reveals that the effective Rashba coefficient decreases more rapidly along the x-axis in the size of 32 × 32. When electron motion is constrained in a smaller region, electron redistribution under the effective magnetic field is more difficult.

The spatial variation of the Rashba coefficient in nanomaterials has a crucial impact on the performance of spin transistors[1,2,5,6,7]. According to Bindel, J., Pezzotta et al[7], the Rashba coefficient of the InSb-based material fluctuates by about 75% in the presence of ~ 1% heavy ions. Since the Rashba coefficients of the InSb-based materials and the Graphene/Nickel(1 1 1) substrate are comparable [7,9], the

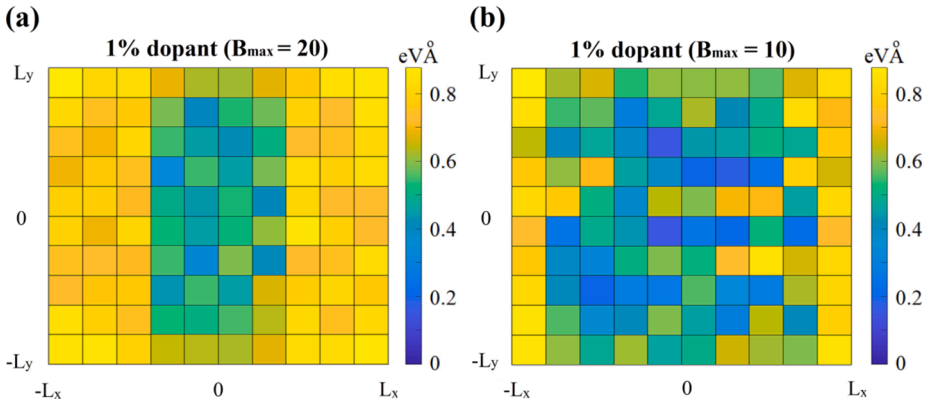

Fig. 6. The real-space patterns of the Rashba coefficient in the Graphene-based materials for different B_{max}. These two samples are at 300 K with the $\alpha_{initial}$ of 1eVÅ. (a) ~ 1% dopants ($Z_{dope} = 50$) are introduced into the sample under a strong E-field screening environment. (b) ~ 1% dopants ($Z_{dope} = 50$) are added into the sample under a weak E-field screening environment.

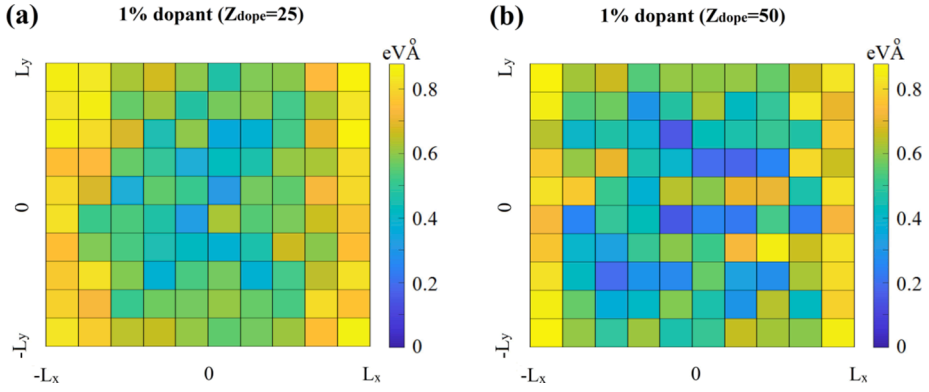

Fig. 7. The real-space patterns of the Rashba coefficient in the Graphene-based materials for various Z_{dope}. These two samples are at 300 K with $B_{max} = 10$ and $\alpha_{initial} = 1$eVÅ. (a) 1% dopants ($Z_{dope} = 25$) are introduced into the sample (b) 1% dopants ($Z_{dope} = 50$) are added into the sample.

ferromagnetic fluctuations of the InSb-based materials at X ~ $\pm L_x$ should also affect the Rashba coefficient about 5% along the sample surface. Hence, for the InSb-based materials, the effect of the sidewalls is not strong enough to compete with the impacts of heavy ions. This may explain why the InSb-based material does not show the dip-like feature when the Rashba parameter is probed at the nanometre scale[7]. Electron-electron interactions in heavy metals are always complex including the InSb-based composite. This may raise a concern if the randomized Rashba parameter is originated from the sophisticated electron–electron interactions in indium (In) and Antimony (Sb) under a strong E-field from dopants. However, our work demonstrates that the fluctuation of the Rashba parameter can occur in a light-element system of graphene in the presence of a strong local E-field emitted by dopants, where the role of nickel substrate is to strengthen the exchange interaction of graphene only. In other words, the complicated electron–electron interaction between the heavy metals and dopants is not the most dominant factor in triggering the randomized Rashba parameter, and that's why we study the Rashba effect of the Graphene/Nickel composite instead of the InSb-based materials. Our model helps figure out the scientific parameters to understand the physics behind the Rashba parameter in nanomaterials.

Fig. 6 supports that the use of 1% heavy dopants with a suitable screening effect is sufficient to randomize the Rashba coefficients along the surface. The screening factor B_{max} and the random number R_{screen} are the calibrated parameters to control the effectiveness of E-field screening, since the point-charge approach may not describe the doped system well. When B_{max} is large, most of the electrons do not experience the E-field emitted from the heavy dopants to a large extent. In other words, the doping term is not dominant in the Hamiltonian. We keep the doping concentration as low as possible because a different algorithm may be required to estimate the effective wavevectors $\langle k_x \rangle$ and $\langle k_y \rangle$ in the over-doped case. After the Rashba effect is activated in our simulation, the mean-field approximation may not be the best option to handle the screening effect since the electron gases are not uniform along the XY plane. Therefore, we assign a random term R_{screen}/B_{max} to mimic the screening effect stochastically and make the simulation data closer to reality.

Our model was developed from the metropolis algorithm of the Ising model, where the spin is fixed in location [23]. To make the simulation more realistic, we include a random number R_{KE} in the kinetic energy term to represent the chaotic motion of electrons. The wavevectors are converted from the experimental Fermi energy and corrected by the DFT calculation, which already contains the lattice potential information, so it is not necessary to add the lattice potential to the Hamiltonian again. After multiplying the wavevector by R_{KE}, the trial wavevector at each Monte Carlo step is accepted if the final energy is less positive (or more negative) than the initial energy. Monte Carlo simulation requires the monitoring of the stochastic variables to reach an equilibrium state [13]. When the effective mass of the electrons is assigned, it prohibits the use of R_{KE}, which is contrary to the nature of Monte Carlo simulation[13]. Otherwise, the initial and final kinetic energies (without R_{KE}) are always the same, and the Monte Carlo system may then have difficulty reaching a ground state. The effective mass of the Graphene/Nickel (1 1 1) substrate is 0.6 m_0, so the kinetic energy term can be kept in non-relativistic form [15]. The momentum of the electrons is always non-zero due to the uncertainty principle. However, our simulation results do not show a noticeable difference when we insert a minimum momentum in the Hamiltonian, since the offset between the initial and final kinetic

energies cancels out two minimum momentum terms.

Let us compare the Hamiltonian in different situations. The first term in the Hamiltonian, the kinetic energy, must be positive. When electrons obey spin-momentum locking, the Hamiltonian is less positive. To favor the Rashba effect (the second term), securing the spin-momentum locking causes the Rashba energy term to be negative. For example, the E_{Rashba} equals to $-\alpha k R_{KE}$ if the spin-up (spin-down) state and positive (negative) k direction are detected. Otherwise, the E_{Rashba} equals to$\alpha k R_{KE}$.

On the other hand, the exchange energy (the third term) is in ferromagnetic nature. The Rashba effect triggers the phenomenon of spin-splitting. At the upper (lower) edge, nearly all electrons are in spin-up state (spin-down state) and therefore the exchange energy term along the Rashba edges prefers to make the Hamiltonian less positive. In addition, the distance between the top and bottom edges is very large. The anti-parallel spin alignment between these two edges has no appreciable effect on the exchange energy term due to the exponential decay of$e^{-\frac{|r_i - r_j|}{r_0}}$.

Dopants contribute a negative energy term that may allow the Hamiltonian to accept unexpected trial states. These unexpected trial states destroy the spin-momentum locking. Without proper spin-momentum locking, the selected electron enters interior regions. The destruction of spin-momentum blocking is illustrated by comparing the Rashba energy and the doping energy. The Rashba wavevector contributes an additional energy of $\frac{\hbar^2 k_{so}^2}{2m} = 0.02$ eV or ($\alpha k_{SO} \sim 0.08$ eV) approximately. This additional energy is comparable to the doping energy when the atomic number of dopants is large. Let us assume that the randomly generated electron-dopant separation is 10 nm. For Z = 50 and $B_{max} = 20$, the doping energy $-\frac{Zq^2}{4\pi\varepsilon dB_{max}}$ corresponds to ~ -0.3 eV. Under these circumstances, the sum of the doping energy and the Rashba energy is negative, therefore the trial states can be unexpectedly accepted. As a result, the spin-momentum locking is suppressed causing the Rashba parameters to fluctuate. In contrast, the exchange energy term cannot destroy the spin-momentum locking because the exchange energy is only on the order of −0.01 eV.

Controlling the spin-orbital coupling of semiconductors is of critically importance for the design of the nanoscale spin-FETs [6]. Although the Rashba coefficient of the InSb-based material is large [7], it is difficult to maintain a constant rate of spin precession across the semiconductor channel due to the randomly fluctuating Rashba coefficient. The use of nano-sized graphene should be able to generate a stable drain current since the spatial dependence of the Rashba coefficient is only ~ 5% (see Fig. 4b). The critical energy barrier [18] is not considered in our model, which implies that the size of the simulation box is much larger than the quantum dot. The exact value of the strain applied to the Nickel (1 1 1) substrate is not important since we want to find a logical argument to lower the initial Rashba coefficient only.

Conclusions

We have developed a Monte Carlo model to tune the spatial variation of the Rashba parameter by controlling the lattice size, atomic number of dopants, dopant concentration, E-field screening, exchange fluctuations, and temperature. Our Monte Carlo model is able to predict the room-temperature Rashba effect in a Graphene/Nickel(1 1 1) substrate, which is consistent with experimental observations. Our simulation not only confirms the role of heavy elements on the Rashba parameter, but also presents a way to predict and suppress the spatial pattern of the Rashba parameter, which is crucial for developing the next-generation spintronic devices and quantum technologies.

CRediT authorship contribution statement

C.H. Wong: Conceptualization, Methodology, Software, Writing – original draft, Writing – review & editing. **R. Lortz:** Writing – original draft, Writing – review & editing, Supervision. **C.Y. Tang:** Writing – review & editing, Supervision. **A.F. Zatsepin:** Writing – review & editing, Supervision.

Declaration of Competing Interest

The authors declare that they have no known competing financial interests or personal relationships that could have appeared to influence the work reported in this paper.

Acknowledgments:

The study was supported by Research Institute for Advanced Manufacturing and the grants from the Research Grants Council of the Hong Kong Special Administrative Region, China (GRF-16302018 & C6025-19G-A). This work was partially supported by the Research Committee of The Hong Kong Polytechnic University under Project Code G-UAMY.

References:

[1] Maaß H, Bentmann H, Seibel C, Tusche C, Eremeev SV, Peixoto TRF, et al. Spin-texture inversion in the giant Rashba semiconductor BiTeI. Nat Commun 2016;7:11621.
[2] Di Sante D, Barone P, Bertacco R, Picozzi S. Electric Control of the Giant Rashba Effect in Bulk GeTe. Advanced Mat 2012;25:509–13.
[3] Rader O, Bihlmayer G, Winkler R. Focus on the Rashba effect. New J Phys 2015;17:050202.
[4] Manchon A, Koo HC, Nitta J, Frolov SM, Duine RA. New perspectives for Rashba spin–orbit coupling. Nat Mater 2015;14:871–82.
[5] Gefei Wang; Zhaohao Wang; Jacques-Olivier Klein; Weisheng Zhao, Modeling for Spin-FET and Design of Spin-FET-Based Logic Gates, IEEE Transactions on Magnetics, Volume: 53, Issue: 11, 1600106 (2017).
[6] Yan W, Txoperena O, Llopis R, Dery H, Hueso LE, Casanova F. A two-dimensional spin field-effect switch, Nature Communications, Volume 7. Article number 2016;13372.
[7] Jan Raphael Bindel, Mike Pezzotta, Jascha Ulrich, Marcus Liebmann, Eugene Ya. Sherman & Markus Morgenstern, Probing variations of the Rashba spin–orbit coupling at the nanometre scale, Nature Physics, Volume 12, Pages 920–925 (2016).
[8] Yamashita T, Lee J, Habe T, Asano Y. Proximity effect in a ferromagnetic semiconductor with spin-orbit interactions. Phys Rev B 2019;100:094501.
[9] Y. S. Dedkov, M. Fonin, U. Rüdiger, C. Laubscha, Rashba Effect in the Graphene/Ni (111) System, Phys. Rev. Lett, 100, 107602 (2008).
[10] Chen Ji. Mansoor Bin Abdul Jalil and Seng Ghee Tan, Spin torque on the surface of graphene in the presence of spin orbit splitting. AIP Adv 2013;3:062127.
[11] Kittel C. Introduction to solid state physics, ISBN-13: 978–0471415268. Wiley; 2004.
[12] Ambrosetti A, Pederiva F, Lipparini E, Gandolfi S. Quantum Monte Carlo study of the two-dimensional electron gas in presence of Rashba interaction. Phys Rev B 2009;80:125306.
[13] Montroll Elliott W. Potts, Renfrey B, Ward, John C. Correlations and spontaneous magnetization of the two-dimensional Ising model, Journal of Mathematical Physics 1963;4(2):308–22.
[14] Wong CH, Buntov EA, Rychkov VN, Guseva MB, Zatsepin AF. Simulation of chemical bond distributions and phase transformation in carbon chains. Carbon 2017;114:106–10.
[15] Achilli S, Tognolini S, Fava E, Ponzoni S, Drera G, Cepek C, et al. Surface states characterization in the strongly interacting graphene/Ni(111) system. New J Phys 2018;20:103039.
[16] Peng H, Perdew JP. Rehabilitation of the Perdew-Burke-Ernzerhof generalized gradient approximation for layered materials. Phys Rev B 2017;95:081105(R).
[17] Yasinskaya DN, Ulitko VA, Chikov AA, Panov YD. Critical Behavior of a 2D Spin-Pseudospin Model in a Strong Exchange Limit. Acta Phys Pol A 2020;137(5):979.
[18] Li R, Liu Z-H, Yidong Wu, Liu CS. The impacts of the quantum-dot confining potential on the spin-orbit effect, Scientific Reports, Volume 8, Article 2018; number:7400.
[19] Ma Y, Dai Y, Yin N, Jing T, Huang B. Ideal two-dimensional systems with a gain Rashba-type spin splitting: SrFBiS2 and BiOBiS2 nanosheets. J Mater Chem C 2014;2:8539–45.
[20] Leontiadou MA, Litvinenko KL, Gilbertson AM, Pidgeon CR, Branford WR, Cohen LF, et al. Experimental determination of the Rashba coefficient in InSb/InAlSb quantum wells at zero magnetic field and elevated temperatures. J Phys: Condens Matter 2011;23(3):035801.

[21] Eldridge PS, Leyland WJH, Lagoudakis PG, Karimov OZ, Henini M, Taylor D, et al. All-optical measurement of Rashba coefficient in quantum wells. Phys Rev B 2008; 77:125344.
[22] Richter M, Carmele A, Butscher S, Bücking N, Milde F, Kratzer P, et al. Two-dimensional electron gases: Theory of ultrafast dynamics of electron-phonon interactions in graphene, surfaces, and quantum wells. J Appl Phys 2009;105: 122409.
[23] Wolf WP. The Ising model and real magnetic materials. Braz J Phys 2000;30(4): 794–810.